

The Crystal and Molecular Structure of Chloro- $\alpha,\beta,\gamma,\delta$ -tetraphenylporphinatomanganese(III)

A. Tulinsky* and Betty M. L. Chen

Contribution from the Department of Chemistry, Michigan State University, East Lansing, Michigan 48824. Received August 6, 1976

Abstract: The x-ray crystallographic structure of chloro- $\alpha,\beta,\gamma,\delta$ -tetraphenylporphinatomanganese(III) was solved by the heavy atom method. The manganese atom shows a slightly distorted square pyramidal coordination with the counter chloride ion in the apical position. The porphine ring system is markedly nonplanar and displays quasi- S_4 -4 symmetry with the pyrrole rings being tilted alternately up and down. The manganese is displaced 0.27 Å from the plane of the pyrrole nitrogens toward the chloride to compensate for a stress caused by the close contacts of the nitrogens and the chloride. The bond angles of the averaged structure correspond to those of the azapyrrole of the free base while the bond distances resemble more those of the reduced pyrrole. An acetone molecule of solvation is located between adjacent molecules interacting with a phenyl group and the chloride ion.

Since manganese is essential in the energy converting unit of the plant^{1,2} and since porphyrins are integral constituents thereof, manganese porphyrins have long been considered to be important in chloroplasts. The evidence for the manganese involvement is that the plant can restore its ability to reduce carbon dioxide and evolve oxygen by adding the ion back to the energy system; however, the evidence implicating the function and environment of manganese is not nearly as clear. Nonetheless, it has been suggested that manganese is complexed with ligands of biological moieties such as porphyrins.³

Physical and chemical properties of manganese porphyrins have been studied comprehensively by Boucher.^{4,5} Magnetic susceptibility measurements suggest that there is no spin pairing in the manganese(III) complex. Far-infrared spectra show metal-anion stretching absorptions (150–500 cm^{-1}) consistent with the strong binding of an additional ligand in an axial position of the metal. In solution, electronic spectra show that six-coordinated manganese porphyrins are present with various ligands. In addition, it was concluded that manganese porphyrins have significant metal-porphyrin π -bonding. However, the porphyrin-metal d-orbital π interaction is difficult to describe quantitatively and two possible geometries of the molecule have been predicted. One is that of a tetragonal structure with the metal ion in the plane of four pyrrole nitrogen atoms with an axial anion and a solvent molecule at a somewhat larger distance from the metal. The other possibility is that the metal atom is out of the plane of porphyrin and approaching the axial anion.

We wish to report here the structure of a synthetic manganese porphyrin, chloro- $\alpha,\beta,\gamma,\delta$ -tetraphenylporphinatomanganese(III), [(Cl)Mn(TPP)], in our continuing program of studying the effects of metallo-substitution and geometry^{6,7} on the free base structure of the porphine macrocycle⁸ to go along with the structures of $(\text{N}_3)\text{Mn}(\text{CH}_3\text{OH})(\text{TPP})$,⁹ $(\text{N}_3)\text{Mn}(\text{TPP})$,¹⁰ and $(\text{Cl})\text{Mn}(\text{Py})(\text{TPP})$ ¹¹ reported by others.

Experimental Section

Single crystals of $(\text{Cl})\text{Mn}(\text{TPP})$ ^{12,13} were grown by slow evaporation of an acetone solution. A dark purple crystal with dimensions of about $0.25 \times 0.15 \times 0.10$ mm was used for the x-ray crystallographic measurements. Preliminary studies showed that the crystal was monoclinic with unit cell dimensions of $a = 14.588$ (5) Å, $b = 21.765$ (6) Å, $c = 17.023$ (6) Å, and $\beta = 135.62$ (4)° and that the space group was $P2_1/c$. The crystal density was measured by flotation in an aqueous silver nitrate solution and it indicated that there were four molecules per unit cell. The observed density was 1.30 g/cm^3 but the calculated density based on four $(\text{Cl})\text{Mn}(\text{TPP})$ molecules in the unit cell was only 1.23 g/cm^3 . The higher observed molecular weight

(738 instead of 702) suggested the presence of an acetone of solvation.

A set of intensity data was collected, from a crystal mounted on a glass fiber, with a Picker four-circle automatic diffractometer using the moving crystal-moving counter technique. Each reflection was scanned for 2° at $2^\circ/\text{min}$ using $\text{Cu K}\alpha$ radiation with a nickel filter and subsequently scanned similarly with a balanced cobalt filter. The intensities of three standard reflections, which were measured periodically (every 100 reflections, ~ 1 h), remained constant throughout the data collection indicating no misalignment and no radiation decay of the crystal. A total of 3978 reflections were measured within $2\theta \leq 100^\circ$. Eliminating unobserved reflections (average value of systematically absent reflections), systematically absent reflections and redundant reflections gave a total of 2977 unique, observable reflections for the structure determination. The intensities of these reflections were corrected semiempirically for absorption¹⁴ ($\mu = 41.0 \text{ cm}^{-1}$; maximum absorption = 1.70 in low and 1.17 in high order reflections). Lorentz and polarization factors were then applied converting the intensities to a set of relative structure amplitudes.

Structure Analysis. The positions of the manganese atoms in the unit cell were found from the three-dimensional Patterson function. The vector peak due to the Mn–Mn interactions was overwhelming in the Harker section ($v = 1/2$). The remaining atoms in the unit cell were obtained using electron density methods.

An electron density was calculated on the basis of the manganese position. A large peak was found in this map approximately 2.5 Å from the manganese atom and approximately perpendicular to the mean plane of a large number of other peaks. The Harker section also contained a vector due to this large peak which, when compared to the Mn–Mn peak height, corresponded to approximately that of a chlorine atom (14 electrons).

The location of the remaining atoms was accomplished using difference electron densities. A structure factor calculation including the complete molecule with an average isotropic thermal parameter, but excluding hydrogen atoms, gave an R value of 0.235 ($R = \sum |F_o| - |F_c| / \sum |F_o|$).

The structure was refined by the method of least squares. A weighting scheme based on that of Hughes¹⁵ was used: $\sigma(|F_o|) = 0.1|F_o|$ for $|F_o| > 15.0$ and $\sigma(|F_o|) = 2.0$ for $|F_o| \leq 15.0$. After several cycles of refinement in which atomic coordinates and anisotropic temperature factors were varied, R decreased to 0.125.

A difference electron density was computed at this stage and four relatively large peaks ($\sim 3 \text{ e } \text{Å}^{-3}$) were found in the vicinity of the chlorine atom and the porphyrin molecule. From an examination of the distances between these peaks, the corresponding angles, and the peak electron densities, it was concluded that they corresponded to an acetone molecule of solvation, thus removing the discrepancy between the observed and calculated crystal densities of about 40 amu. The R factor increased to 0.129 by including the acetone molecule into a structure factor calculation but after one cycle of refinement of coordinates and anisotropic temperature factors of all the atoms, the R factor decreased spectacularly to 0.085 and further refinement reduced it to 0.078.

Table I. Final Atomic Parameters of (Cl)Mn(TPP)^a

Atom	<i>x</i>	<i>y</i>	<i>z</i>	β_{11}	β_{22}	β_{33}	β_{12}	β_{13}	β_{23}
Mn ^b	0.52272 (9)	0.11500 (4)	0.09000 (8)	67 (12)	11 (2)	56 (9)	2 (4)	47 (9)	2 (3)
Cl ^b	0.62761 (16)	0.16730 (7)	0.25846 (14)	10 (23)	19 (5)	61 (16)	3 (8)	57 (17)	-4 (7)
N1	0.4000 (4)	0.0619 (2)	0.0756 (4)	52 (5)	13 (1)	54 (4)	6 (2)	39 (4)	3 (1)
C11	0.2801 (7)	0.0789 (3)	0.0336 (5)	93 (9)	15 (1)	74 (6)	0 (3)	70 (6)	1 (2)
C12	0.2413 (7)	0.0356 (2)	0.0695 (6)	103 (9)	16 (1)	77 (6)	2 (2)	71 (6)	2 (2)
C13	0.3374 (7)	-0.0074 (2)	0.1328 (6)	78 (9)	16 (1)	81 (6)	0 (2)	62 (6)	0 (2)
C14	0.4342 (7)	0.0077 (3)	0.1351 (5)	68 (9)	15 (1)	54 (6)	-3 (3)	49 (6)	-1 (2)
N2	0.6437 (3)	0.0427 (2)	0.1493 (4)	67 (5)	11 (1)	64 (4)	-0 (2)	51 (4)	-1 (1)
C21	0.6337 (6)	-0.0135 (2)	0.1817 (5)	74 (8)	13 (1)	56 (6)	4 (3)	51 (6)	7 (2)
C22	0.7334 (7)	-0.539 (3)	0.2133 (6)	79 (9)	14 (1)	65 (5)	7 (2)	59 (5)	2 (2)
C23	0.8049 (6)	-0.223 (2)	0.2037 (6)	95 (8)	13 (1)	66 (5)	4 (2)	61 (6)	3 (2)
C24	0.7512 (7)	0.0381 (2)	0.1666 (5)	63 (9)	12 (1)	58 (6)	2 (2)	44 (6)	-2 (3)
N3	0.6266 (4)	0.1595 (3)	0.0721 (4)	67 (5)	12 (1)	53 (4)	3 (2)	46 (4)	4 (1)
C31	0.7493 (7)	0.1448 (2)	0.1195 (5)	63 (9)	16 (1)	57 (6)	0 (3)	48 (6)	-0 (2)
C32	0.8108 (7)	0.1974 (2)	0.1222 (6)	111 (8)	14 (1)	92 (5)	-3 (2)	81 (6)	4 (2)
C33	0.7238 (7)	0.2445 (2)	0.0747 (6)	89 (9)	21 (1)	92 (6)	4 (2)	71 (6)	8 (2)
C34	0.6085 (7)	0.2211 (2)	0.0415 (5)	92 (9)	16 (1)	66 (6)	5 (2)	62 (6)	5 (2)
N4	0.3738 (4)	0.1757 (2)	-0.0161 (4)	63 (5)	13 (1)	63 (4)	4 (2)	49 (4)	-2 (1)
C41	0.2497 (6)	0.1731 (3)	-0.0613 (5)	69 (9)	13 (1)	63 (6)	4 (3)	50 (6)	1 (2)
C42	0.1744 (7)	0.2351 (2)	-0.1335 (6)	73 (9)	19 (1)	72 (6)	9 (2)	49 (6)	-9 (2)
C43	0.2549 (7)	0.2603 (2)	-0.1378 (6)	88 (9)	18 (1)	60 (6)	7 (2)	55 (6)	-6 (2)
C44	0.3810 (7)	0.2305 (3)	-0.0536 (5)	81 (8)	14 (1)	65 (6)	9 (3)	59 (6)	-6 (2)
PH11	0.2046 (6)	0.1296 (3)	-0.0356 (5)	78 (9)	14 (2)	65 (6)	-1 (3)	55 (6)	-3 (2)
PH12	0.0727 (6)	0.1394 (3)	-0.0799 (6)	57 (9)	17 (2)	74 (7)	8 (3)	46 (6)	11 (2)
PH13	-0.0266 (7)	0.0955 (3)	-0.1509 (6)	87 (9)	34 (2)	105 (7)	-2 (3)	72 (7)	-0 (3)
PH14	-0.1521 (6)	0.1136 (4)	-0.1935 (6)	90 (10)	52 (2)	127 (7)	3 (4)	77 (7)	1 (3)
PH15	-0.1754 (7)	0.1560 (3)	-0.1648 (8)	117 (10)	40 (2)	160 (7)	22 (4)	111 (7)	5 (3)
PH16	-0.0753 (7)	0.1996 (3)	-0.0921 (7)	157 (9)	37 (2)	190 (7)	17 (3)	154 (6)	6 (3)
PH17	0.0475 (7)	0.1901 (3)	-0.0488 (6)	123 (9)	23 (2)	125 (6)	7 (3)	100 (6)	0 (2)
PH21	0.5414 (6)	-0.0288 (3)	0.1821 (5)	83 (9)	9 (2)	57 (6)	2 (3)	54 (6)	1 (2)
PH22	0.5612 (6)	-0.0872 (3)	0.2395 (6)	73 (9)	15 (2)	47 (6)	4 (3)	45 (6)	2 (2)
PH23	0.4696 (6)	-0.1341 (3)	0.1875 (7)	117 (9)	12 (3)	85 (6)	2 (3)	82 (6)	3 (3)
PH24	0.4875 (7)	-0.1888 (4)	0.2306 (6)	131 (10)	16 (2)	111 (6)	0 (4)	100 (7)	2 (3)
PH25	0.5963 (7)	-0.1962 (3)	0.3437 (8)	127 (9)	19 (3)	91 (7)	5 (4)	82 (7)	8 (3)
PH26	0.6867 (8)	-0.1502 (3)	0.4048 (7)	126 (9)	23 (2)	95 (7)	6 (3)	75 (6)	13 (3)
PH27	0.6593 (7)	-0.0948 (3)	0.3520 (6)	119 (9)	22 (3)	65 (6)	3 (3)	70 (6)	6 (2)
PH31	0.8071 (6)	0.0864 (3)	0.1575 (5)	61 (8)	15 (2)	53 (6)	2 (3)	44 (6)	2 (2)
PH32	0.9326 (6)	0.0772 (3)	0.1929 (5)	74 (9)	13 (2)	72 (7)	1 (3)	59 (6)	-0 (2)
PH33	0.0460 (6)	0.0598 (3)	0.3016 (6)	64 (9)	23 (3)	76 (7)	7 (3)	42 (6)	4 (3)
PH34	0.1642 (6)	0.0541 (4)	0.3320 (7)	70 (10)	28 (2)	122 (7)	7 (4)	58 (7)	1 (3)
PH35	0.1730 (7)	0.0664 (3)	0.2579 (8)	114 (10)	24 (2)	140 (7)	-0 (4)	101 (7)	-1 (3)
PH36	0.0611 (7)	0.0846 (3)	0.1509 (7)	117 (9)	21 (2)	145 (7)	-1 (3)	110 (6)	-4 (3)
PH37	0.9406 (7)	0.0895 (3)	0.1173 (6)	114 (9)	21 (2)	93 (6)	-3 (3)	84 (7)	-6 (2)
PH41	0.4927 (6)	0.2543 (3)	-0.0192 (5)	95 (9)	15 (2)	80 (6)	7 (3)	75 (6)	6 (2)
PH42	0.4930 (6)	0.3190 (3)	-0.0491 (6)	91 (9)	17 (7)	90 (7)	15 (3)	73 (6)	19 (2)
PH43	0.4717 (9)	0.3320 (3)	-0.1388 (8)	250 (9)	21 (3)	158 (7)	36 (3)	175 (6)	40 (3)
PH44	0.4901 (9)	0.3915 (4)	-0.1568 (8)	232 (10)	34 (2)	161 (7)	44 (4)	168 (7)	32 (3)
PH45	0.5244 (7)	0.4364 (5)	-0.0854 (8)	89 (10)	46 (2)	152 (7)	2 (4)	83 (7)	37 (3)
PH46	0.5412 (9)	0.4254 (4)	0.0041 (9)	198 (9)	25 (2)	128 (7)	-13 (3)	68 (6)	3 (3)
PH47	0.5238 (9)	0.3650 (3)	0.0233 (7)	184 (9)	11 (2)	89 (6)	-13 (3)	70 (7)	-2 (2)

^a Anisotropic temperature factor = $\exp[-(\beta_{11}h^2 + \beta_{22}k^2 + \beta_{33}l^2 + 2\beta_{12}hk + 2\beta_{13}hl + 2\beta_{23}kl)]$; $\beta_{ij} \times 10^4$. ^b Standard deviations of $\beta_{ij} \times 10^5$.

Table II. Atomic Parameters of Acetone Solvate^a

Atom	<i>x</i>	<i>y</i> ^b	<i>z</i>	β_{11}	β_{22}	β_{33}	β_{12}	β_{13}	β_{23}
O1	0.860 (1)	0.038 (5)	0.502 (1)	285 (18)	50 (3)	212 (12)	15 (6)	139 (13)	16 (5)
C2	0.900 (1)	0.086 (5)	0.507 (1)	152 (15)	20 (3)	105 (11)	25 (6)	-13 (11)	27 (5)
C3	0.957 (1)	0.103 (8)	0.462 (1)	192 (16)	92 (4)	113 (12)	54 (6)	133 (17)	28 (6)
C4	0.912 (2)	0.138 (8)	0.568 (1)	320 (17)	67 (3)	110 (12)	-96 (6)	121 (12)	13 (5)

^a $\beta_{ij} \times 10^4$. ^b Standard deviation $\times 10^4$.

Another difference electron density was calculated and all the hydrogen atoms were found at approximately expected locations. The hydrogen atoms were assumed to have isotropic temperature factors about 20% greater than those of their adjacent carbon atoms. After one cycle of refinement on coordinates and anisotropic temperature

factors with all atoms included, the *R* factor was 0.067. Since the acetone molecule seemed not to be at full occupancy, its weight was reduced to 0.75. The *R* factor remained the same and the final weighted *R_w* factor was 0.098 [$R_w = (\sum w(|F_o| - |F_c|)^2) / \sum w|F_o|^2$]^{1/2}. The maximum shift/error and the average shift/error

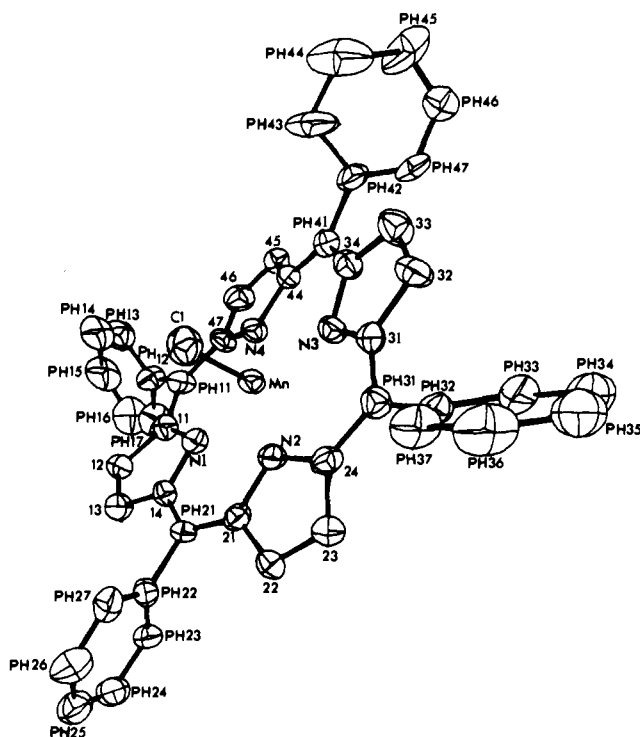


Figure 1. ORTEP drawing and numbering scheme of (Cl)Mn(TPP).

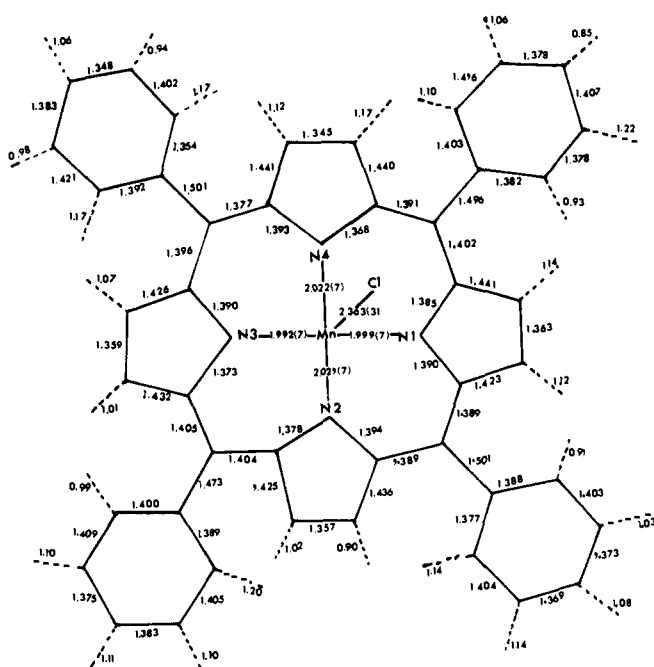


Figure 2. Interatomic distances of (Cl)Mn(TPP). Broken lines are C-H distances.

of the last cycle were about 0.7 (for the acetone) and generally less than 0.3, respectively.

Several of the most intense reflections are probably affected by extinction as judged from discrepancies between observed and calculated structure factors.¹⁶ Since the number of these is very small, no further corrections were applied to compensate for the effect.

Results

The numbering scheme adopted for the atoms of (Cl)Mn(TPP) is shown in Figure 1. The final atomic coordinates and anisotropic temperature factors of the atoms of (Cl)Mn(TPP) are listed in Table I. The coordinates of the hydrogen atoms are given in Table II of the supplementary materi-

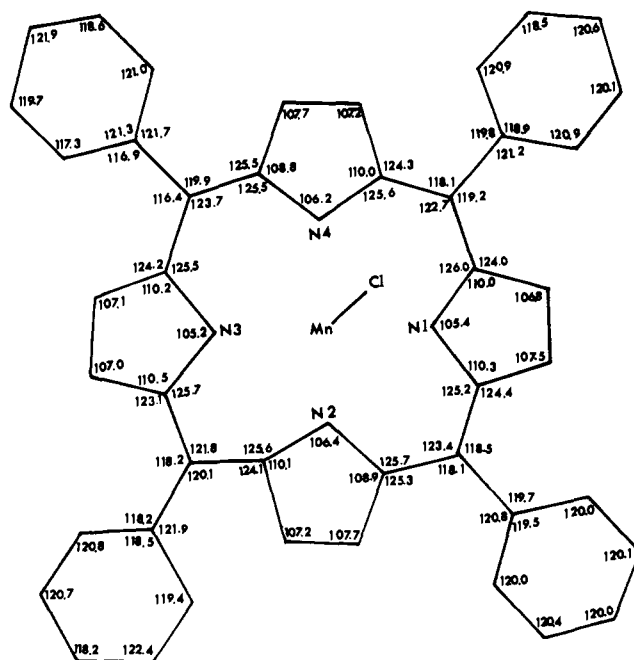


Figure 3. Bond angles of (Cl)Mn(TPP).

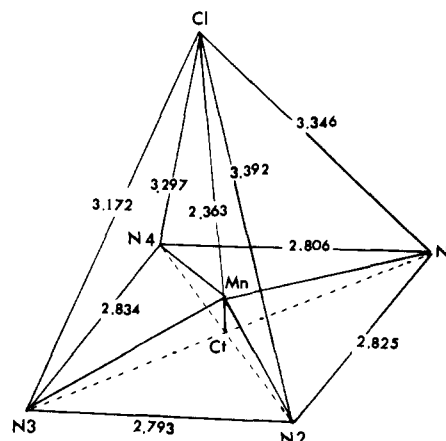


Figure 4. Geometry of the manganese coordination. Bond angles are: $\angle N1, Mn, N3 = 166.9(3)^\circ$; $\angle N2, Mn, N4 = 161.7(3)^\circ$; $\angle N1, Mn, Cl = 100.0(2)^\circ$; $\angle N2, Mn, Cl = 101.0(2)^\circ$; $\angle N3, Mn, Cl = 93.1(2)^\circ$; $\angle N4, Mn, Cl = 97.2(2)^\circ$.

al,¹⁶ while the atomic parameters of the acetone molecule of solvation are listed in Table II. Various interatomic distances of (Cl)Mn(TPP) are presented in Figure 2, with corresponding bond angles shown in Figure 3. Other bond distances and angles involving the manganese atom are shown in Figure 4. The errors in the bond distances based on the standard deviations of the atomic coordinates of the final cycle of refinement range from 0.008 to 0.009 Å for the pyrrole rings and up to 0.013 Å for some of the distances in the phenyl rings; the standard deviations in bond angles are 0.4–0.7°.

Pertinent data relating to the nuclear least-squares (NLS) plane of the macrocyclic, the pyrrole, and the phenyl rings of (Cl)Mn(TPP) are given in Table III of the supplementary material.¹⁶ The standard deviations of atoms from the calculated least-squares planes of the different planar moieties of (Cl)Mn(TPP) averaged from 0.007 to 0.016 Å. The deviation of each atom of the porphyrin ring from the NLS plane is shown in Figure 5. The standard deviation of the NLS plane is about ± 0.03 Å. The dihedral angles between the NLS plane and the individual pyrroles are 1 = +9.2°, 2 = -10.5°, 3 = +9.4°, and 4 = -9.4°, the corresponding angles of the individual phenyl

Table III. Comparison of Some Averaged Mn(TPP) Structures with Averaged Free Base Structure^a

Bond ^b	(Cl)Mn(TPP)	(Cl)Mn(Py)(TPP)	(N ₃)Mn(TPP)	(N ₃)Mn(CH ₃ OH)(TPP)	Av free base ⁸	
					Azapyrrole	Reduced pyrrole
N-C _a	1.384 (11)	1.344 (5)	1.385 (6)	1.376 (8)	1.378 (10)	1.378 (4)
C _a -C _b	1.433 (7)	1.437 (5)	1.430 (4)	1.436 (8)	1.451 (9)	1.432 (6)
C _b -C _b	1.356 (7)	1.351 (2)	1.345 (7)	1.345 (2)	1.345 (3)	1.360 (10)
C _a -C _m	1.394 (9)	1.396 (4)	1.393 (4)	1.394 (7)	1.398 (4)	
Angle						
CaNCa	105.8 (5)	106.6 (4)	106.0 (1)	106.4 (2)	106.3 (3)	109.1 (6)
NC _a C _b	109.9 (6)	109.4 (3)	109.4 (4)	109.4 (4)	109.8 (4)	107.5 (7)
C _a C _b C _b	107.3 (3)	107.3 (4)	107.6 (3)	107.4 (4)	107.1 (7)	108.0 (4)
C _m C _a	122.9 (7)	123.6 (3)	123.2 (1)	123.7 (3)	125.6 (3)	

^a Standard deviations are from averaged value (assuming the same population). ^b Nomenclature according to H. L. Hoard, *Science*, **174**, 1295 (1971).

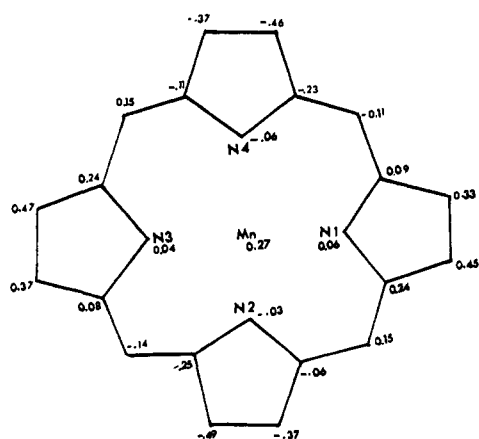


Figure 5. Deviations of the atoms (Å) from the nuclear least-squares plane.

groups are 1 = 54.2°, 2 = 123.5°, 3 = 49.7°, and 4 = 77.4° while that of the Mn-Cl line is 85.3°.

Discussion

The fourfold averaged structure of the porphine macrocycle of (Cl)Mn(TPP) is listed in Table III, where it is compared with the averaged porphine structure of (Cl)Mn(Py)(TPP),¹¹ (N₃)Mn(TPP),¹⁷ and (N₃)Mn(CH₃OH)(TPP).¹⁷ From Table III, it will be seen that the four related structures are the same within the error of their determination. In addition, Table III, lists the averaged structures of the aza and reduced pyrrole rings of the free base macrocycle.⁸ A comparison of the latter with the averaged manganese structures reveals an interesting relationship: the averaged bond distances of the manganese structures tend toward those of the reduced pyrrole whereas the averaged bond angles approximate those of the aza ring. The correspondence of the more sensitive measure of bond angles is as expected with metallo-substitution; however, the significance of the bond distance trend is not nearly as clear.

From Figure 5, it can be seen that the porphine ring system of (Cl)Mn(TPP) is markedly nonplanar showing deviations from the NLS plane of up to 0.5 Å. Moreover, the conformational geometry of the macrocyclic ring approximates quasi-S₄-4 symmetry within the error of the determination. This S₄ conformation differs from that observed in some M(TPP) molecules (M = Cu, Pd, Fe, Co, Ni)^{18,19} but is strikingly similar to that observed with the porphyrin diacids, H₄(TPP)²⁺ and H₄(TPyP)²⁺, where all four of the pyrrolic nitrogen atoms are protonated.²⁰ In the case of the latter, the pyrrole rings are tilted alternately up and down with respect to the 4 axis around the C_a-C_m bonds. Such a conformation is ideal for minimizing

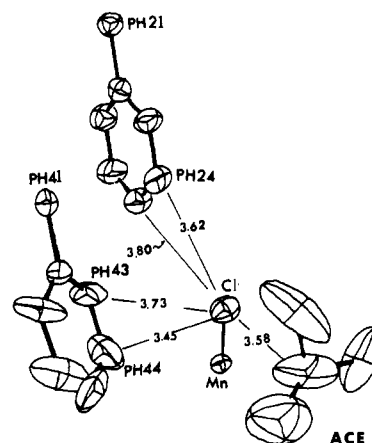


Figure 6. ORTEP drawing of molecular packing in vicinity of Mn-Cl bond. Acetone of solvation designated as ACE; phenyl ring 2 related to Mn-Cl and ACE by $(x, \frac{1}{2} - y, \frac{1}{2} + z)$; phenyl 4 by $(\bar{x}, \frac{1}{2} + y, \frac{1}{2} - z)$.

the repulsive interactions of the four inner hydrogen atoms in the diacid structures. However, with (Cl)Mn(TPP), the reasons for the symmetry of the nonplanarity seem much more obscure even though (N₃)Mn(TPP) shows a similar ruffling.¹⁷

The distorted square pyramidal geometry of the manganese coordination is shown in Figure 4. The manganese atom is displaced 0.27 Å from the plane of the pyrrolic nitrogen atoms in the direction of the counter chloride ion. Hoard had discussed in a review¹⁸ the averaged geometry of the central core region of (Cl)Mn(TPP) pointing out that the Cl-N_p distance of 3.30 Å is slightly shorter (0.2 Å) than the sum of the van der Waals radii of these atoms leading to a lengthening of the axial bond. In fact, it can be seen from Figure 4 that this van der Waals contact is as small as 3.17 Å. The Mn-Cl distance is about 0.16 Å longer than the corresponding Fe-Cl bond in chlorohemin. A much smaller difference would be expected on the basis of the difference in nuclear charges of the atoms. Thus, in view of the relatively strong Mn-N_p bonds (2.008 Å compared to 2.04 Å expected of covalent radii), all or most of the displacement of the manganese atom from the plane of the nitrogens is probably a compensation of the stress caused by the relatively close packing contacts of the nitrogens and the chloride ion. Moreover, the S₄ ruffling of the porphine ring is probably also related to the displacement. Lastly, the 2.363 Å distance of Mn-Cl suggests an appreciable amount of covalent character to the bond.

The Mn-Cl direction makes a small angle with respect to the normal to the plane of the nitrogen atoms (4.7°) in the direction of N3 (Figure 4). An examination of the environment of the chloride ion (Figure 6) shows that it is surrounded by

two phenyl groups from two different adjacent molecules and an acetone molecule of solvation. If the Mn–Cl direction corresponded with the normal to the plane of the nitrogens, the contact between PH44 and the chloride would be prohibitively close. Thus, the distortion of the square pyramidal symmetry appears to be the result of a compromise between molecular packing constraints. In fact, since three of the phenyl groups are inclined about 50° to the NLS plane while the one making the close contact with the chloride is inclined 77° would seem to indicate that the rotation of this phenyl group is also participating in the compromise.

The anisotropic temperature factors of the (Cl)Mn(TPP) (Table I) generally increase as the distance of the atoms increases from the center of the molecule. Such behavior has been observed previously with TPP²¹ and (H₂O)Mg(TPP)²² and is due to a small quasi-rigid body angular oscillation of the molecule. Thus, the peripheral atoms of the molecule have reduced peak heights and consequently, increased standard deviations in atomic parameters.

Acknowledgment. We would like to thank Professor V. W. Day, Department of Chemistry, University of Nebraska, Lincoln, Nebraska for providing us with the results of some Mn(TPP) structure determinations prior to publication. Acknowledgment is made to donors of the Petroleum Research Fund, administered by the American Chemical Society, for the support of this research.

Supplementary Material Available: A table of $|F_o|$ and $|F_c|$ (Table I), hydrogen atom coordinates (Table II), and parameters of least-squares planes (Table III) (9 pages). Ordering information is given on any current masthead page.

References and Notes

- (1) P. A. Loach and M. Calvin, *Biochemistry*, **2**, 361 (1963).
- (2) P. A. Loach and M. Calvin, *Nature (London)*, **202**, 343 (1964).
- (3) M. Calvin, *Rev. Pure Appl. Chem.*, **15**, 1 (1965).
- (4) L. J. Boucher, *J. Am. Chem. Soc.*, **90**, 6640 (1968).
- (5) L. J. Boucher, *Coord. Chem. Rev.*, **7**, 289 (1972).
- (6) I. Moustakali and A. Tulinsky, *J. Am. Chem. Soc.*, **95**, 6811 (1973).
- (7) A. Mavridis and A. Tulinsky, *Inorg. Chem.*, **15**, 2723 (1976).
- (8) P. W. Coddling and A. Tulinsky, *J. Am. Chem. Soc.*, **94**, 4151 (1972).
- (9) V. W. Day, B. R. Stults, E. L. Tasset, R. O. Day, and R. S. Marianelli, *J. Am. Chem. Soc.*, **96**, 2650 (1974).
- (10) V. W. Day, B. R. Stults, E. L. Tasset, R. S. Marianelli, and L. J. Boucher, *Inorg. Nucl. Chem. Lett.*, **11**, 505 (1975).
- (11) J. F. Kirner and W. R. Scheidt, *Inorg. Chem.*, **14**, 2081 (1975).
- (12) We would like to thank Dr. A. D. Adler for kindly supplying us with a sample of this compound.
- (13) A. D. Adler, F. R. Longo, F. Kampas, and J. Kim, *J. Inorg. Nucl. Chem.*, **32**, 2443 (1970).
- (14) A. C. T. North, D. C. Phillips, and F. S. Mathews, *Acta Crystallogr., Sect. A*, **24**, 351 (1968).
- (15) E. W. Hughes, *J. Am. Chem. Soc.*, **63**, 1737 (1941).
- (16) See paragraph at end of paper regarding supplementary material.
- (17) V. W. Day, private communication.
- (18) J. L. Hoard in "Porphyrins and Metalloporphyrins", K. M. Smith, Ed., Elsevier, Amsterdam, 1975, p 317f.
- (19) E. B. Fleischer, C. K. Miller, and L. E. Webb, *J. Am. Chem. Soc.*, **86**, 2342 (1964).
- (20) A. Stone and E. B. Fleischer, *J. Am. Chem. Soc.*, **90**, 2735 (1968).
- (21) S. J. Sivers and A. Tulinsky, *J. Am. Chem. Soc.*, **89**, 3331 (1967).
- (22) R. Timkovich and A. Tulinsky, *J. Am. Chem. Soc.*, **91**, 4430 (1969).

Interaction of Metal Ions with 8-Azapurines. 3. Synthesis and Structure of Trichloro(8-azaadeninium)zinc(II).

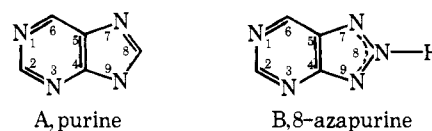
Linda Goodrich Purnell and Derek J. Hodgson*

Contribution from the Department of Chemistry, The University of North Carolina, Chapel Hill, North Carolina 27514. Received June 28, 1976

Abstract: The complex trichloro(8-azaadeninium)zinc(II), [ZnCl₃(AAH)], C₄H₅Cl₃N₆Zn, has been synthesized, and its crystal and molecular structure have been determined from three-dimensional x-ray counter data. The complex crystallizes in the triclinic space group *P* $\bar{1}$ with two molecules in a cell of dimensions: $a = 6.516$ (16), $b = 10.389$ (25), $c = 7.736$ (17) Å; $\alpha = 107.13$ (12), $\beta = 86.01$ (11), $\gamma = 93.31$ (11)°. The observed and calculated densities are 2.03 (3) and 2.056 g cm⁻³, respectively. Least-squares refinement of 746 data obtained from a crystal of poor quality has led to a conventional *R* factor (on *F*) of 0.073. The structure consists of monomeric [ZnCl₃(AAH)] units which are hydrogen bonded to each other. The zinc(II) ion coordinates to the azapurine cation through the N(3) atom only with a Zn–N bond length of 2.07 (1) Å. This type of coordination is unique for purines and their analogues. The geometry around the zinc(II) center is roughly tetrahedral, the three remaining sites being occupied by chloride ions at distances of 2.215 (5) to 2.267 (5) Å. The purine ring is protonated at N(1), C(2), and N(8) only. There is no intramolecular hydrogen bonding, but the intermolecular hydrogen bonding is extensive. The geometry of the azapurine ligand is consistent with that observed in other studies.

A recent review¹ of crystallographic studies of metal–purine complexes has revealed two basic trends concerning the site of metal coordination. In the majority of cases, if the purine (A) is substituted in the N(9) position, the metal will coordinate to N(7); the only known exception to this rule occurs² in the trichloro(9-methyladenine)zincate(II) ion, [ZnCl₃(9MA)]⁻, where the metal coordinates to N(1). In unsubstituted purines, the metal will coordinate to the imidazole nitrogen which is protonated in the free neutral ligand (N(7) for theophylline and N(9) for all other naturally occurring purines¹); the only known exception to this rule is³ trichloro(adeninium)zinc(II), [ZnCl₃(AH)], where the metal

coordinates to N(7). The N(9) position in this compound is protonated.



Since some of the 8-azapurines (B) are known to be of chemotherapeutic value,^{4,5} metal interactions with these purine analogues have been of considerable interest in our laboratory. Crystallographic⁶ and chemical^{7,8} studies of 8-azapurine nu-